Three-Dimensional Reluctance Network Analysis Considering an Iron Loss Characteristic for an EIE-Core Variable Inductor

Kenji Nakamura[1], *Member, IEEE*, Shuichi Hayakawa[1], Shigeaki Akatsuka[2], Takashi Ohinata[2], Kazuo Minazawa[2], and Osamu Ichinokura[1], *Member, IEEE*

[1]Graduate School of Engineering, Tohoku University, Aoba-ku, Sendai 980-8579, Japan
[2]Tohoku Electric Power Company Inc., Aoba-ku, Sendai 980-8550, 981-0952 Japan

This paper presents a quantitative analysis method for an EIE-core variable inductor, which is applied as a voltage regulator in an electric power system. We propose a three-dimensional nonlinear reluctance network analysis (RNA) model of an EIE-core considering magnetic hysteresis. The RNA model of the core is coupled with external electric circuits, in order to simulate an EIE-core variable inductor. Using the coupled model, we can calculate the operating characteristics of the variable inductor including an iron loss. Furthermore, we describe the development of a trial 6.6 kV–300 kVA reactive power compensator using an EIE-core.

***Index Terms*—Coupled analysis, EIE-core, iron loss, reactive power compensator, reluctance network analysis (RNA), variable inductor.**

I. Introduction

IN ELECTRIC power systems, the importance of stabilizing a line voltage has been increasing as a result of the variability of loads. One method of regulating the voltage is control of the reactive power in an electric power system. Static var compensators (SVCs) and static var generators (SVGs), which are one of the semiconductor power converters, have been introduced for this purpose [1], [2]. These apparatuses, however, have various problems such as harmonic current, electromagnetic interference (EMI), and high cost.

Another effective device for reactive power control is a variable inductor [3], [4]. It consists of a magnetic core and windings, and can change its winding inductance by utilizing the nonlinear B-H characteristic of cores. Since the variable inductor has desirable features such as a simple and robust structure and high reliability, it is a suitable apparatus for reactive power compensation in an electric power system.

Though a problem of harmonic currents, due to the nonlinear magnetization, has been pointed out, we have proposed an orthogonal-core variable inductor with wedge gaps on a contact surface of c-cores [5]. We have developed a trial 100-kVA reactive power compensator using the orthogonal-core, and indicated that the trial compensator has good controllability and an almost sinusoidal current. The orthogonal-core, however, has a capacity limit, because the manufacture of a large scale c-core is difficult in general.

In this paper, we present a novel variable inductor using an EIE-core, which is suitable for a larger capacity because the core is made of laminated iron and has no gaps for harmonic current reduction. We propose a quantitative analysis method of the operating characteristics of the EIE-core variable inductor considering an iron loss. The proposed method is based on a three-dimensional (3-D) nonlinear reluctance network analysis (RNA). Furthermore, we present the development of a trial 6.6-kV–300-kVA variable inductor using the EIE-core.

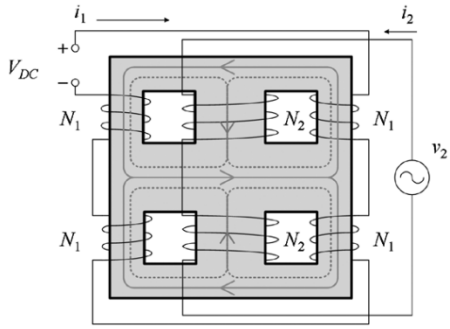

Fig. 1. Schematic diagram of the EIE-core variable inductor.

II. Reluctance Network Analysis Considering Magnetic Hysteresis

Fig. 1 shows a schematic diagram of an EIE-core variable inductor. In the figure, the primary windings N_1 are connected to the direct current (dc) voltage source V_{DC}. The secondary windings N_2 are coiled around the center legs and connected to the sinusoidal power supply v_2. The solid lines indicate primary fluxes and the dotted lines secondary fluxes. The reluctance of the common magnetic path can be changed by the primary dc excitation due to the nonlinear B-H characteristic of the core. Accordingly, the effective inductance of the secondary windings is controlled by the primary dc current.

Since the variable inductor changes its secondary winding inductance by utilizing the nonlinear B-H characteristic, magnetic saturation and ensuing flux leakage occur. Thus, 3-D nonlinear magnetic field analysis is needed for optimum design of the core. A coupled analysis of the core and external electric circuits is also needed to calculate the operating characteristics of the variable inductor.

Digital Object Identifier 10.1109/TMAG.2005.854990

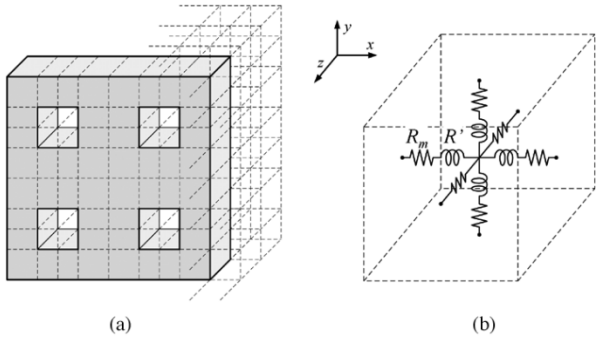

Fig. 2. Reluctance network analysis model of an EIE-core. (a) Division of the core. (b) 3-D magnetic circuit.

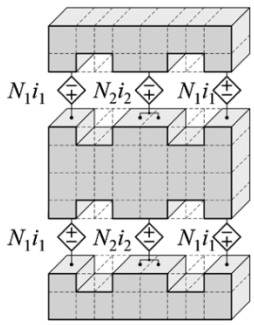

Fig. 3. Arrangement of MMF sources.

In this paper, we employed the RNA for the calculation. The RNA is suitable for dynamic simulations of a variable inductor because of its simple modeling, high calculation accuracy, and ease of coupled analysis [6], [7].

First, we divide an EIE-core into multiple elements, as shown in Fig. 2(a). To allow consideration of leakage fluxes, the surrounding space is also divided. The divided elements can be expressed by a 3-D magnetic circuit, as shown in Fig. 2(b). In the magnetic circuit, a relationship between the magnetomotive force (MMF) f_m and the flux ϕ is expressed as follows:

$$f_m = R_m\phi + R'\frac{d\phi}{dt} = \left(\frac{\alpha_1 l}{S} + \frac{\alpha_n l}{S^n}\phi^{n-1}\right)\phi + \left\{\frac{\beta_1 l}{S} + \frac{\beta_m l}{S^m}\left(\frac{d\phi}{dt}\right)^{m-1}\right\}\frac{d\phi}{dt} \quad (1)$$

where the coefficients are α_1 and $\alpha_{\rm n}$, which are determined by the B-H curve of the core material, and the iron loss characteristic gives the coefficients β_1 and $\beta_{\rm m}$. The coefficients using the analysis are $\alpha_1 = 65$ A/m·T, $\alpha_{13} = 5.1$ A/m·T^{13}, $\beta_1 = 0.12$ A·s/m·T, and $\beta_9 = 3.6 \times 10^{-24}$ A·s^9/m·T^9, respectively. On the other hand, the reluctance in the surrounding space is determined by a permeability of free space μ_0. The MMF sources N_1i_1, N_2i_2 exerted by the winding currents are set in the center of each leg, as shown in Fig. 3.

Using the 3-D nonlinear RNA model, we can calculate the flux-MMF relationships of the EIE-core. Furthermore, if the RNA model and external electric circuits are coupled by an appropriate method, we can directly calculate the operating characteristics of the variable inductor under dc control.

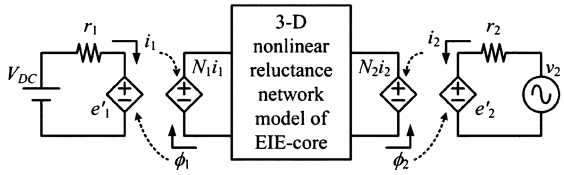

Fig. 4. Electric and magnetic coupled analysis model for the EIE-core variable inductor.

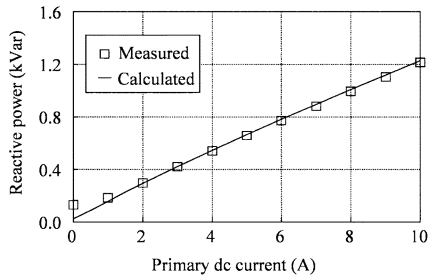

Fig. 5. Measured and calculated control characteristics of the EIE-core variable inductor.

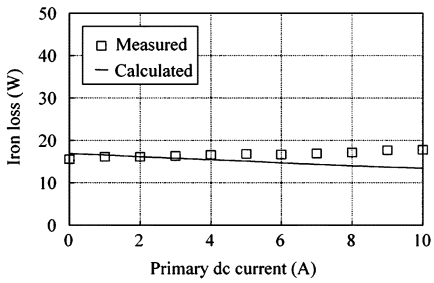

Fig. 6. Measured and calculated iron loss characteristics of the EIE-core variable inductor.

Fig. 4 shows the electric and magnetic coupled analysis model for the EIE-core variable inductor. The primary dc voltage and secondary alternating current (ac) voltage sources are $V_{\rm DC}$ and v_2, respectively. The primary and secondary winding resistances are r_1 and r_2, respectively. In the coupled analysis model, if the currents i_1 and i_2, which present the MMF's N_1i_1 and N_2i_2, are given, we can obtain the primary and secondary fluxes ϕ_1 and ϕ_2 by the 3-D nonlinear RNA model. The fluxes give the induced voltages $e'_1 = N_1(d\phi_1/dt)$ and $e'_2 = N_2(d\phi_2/dt)$, respectively. We can then determine the primary and secondary currents i_1 and i_2 from the electric circuits.

Fig. 5 shows the control characteristics of the EIE-core variable inductor. In the figure, the line is a calculated result and the symbols are measured values. Fig. 6 shows the iron loss characteristics. In the proposed method, the iron loss is obtained from the stored energy of the inductance R' shown in Fig. 2(b). Therefore, the eddy current loss caused by leakage flux passing through the direction of z axis is neglected.

Fig. 7 shows the observed and calculated waveforms of the secondary current when the primary dc current is 10 A. The figures reveal that the calculated results almost agree well with the measured ones.

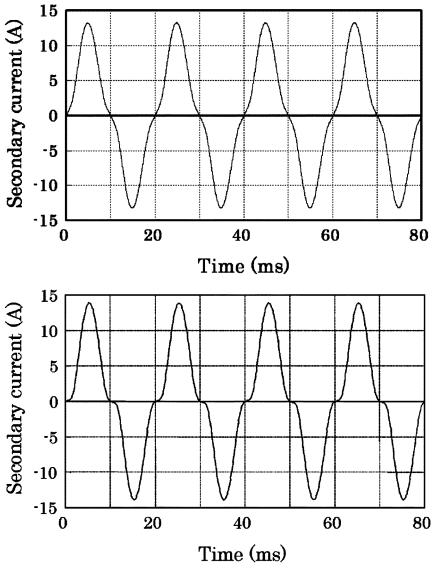

Fig. 7. Waveforms of the secondary current when the primary dc current is 10 A (top: observed; bottom: calculated).

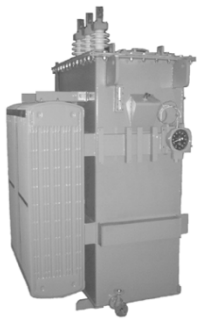

Rated voltage	6.6 kV
Rated capacity	300 kVA
Type	Oil-immersed, self-cooled
Size	W1500 × D1900 × H2300 mm
Weight	3.9 t

Fig. 8. General view of the trial three-phase 6.6-kV-300-kVA reactive power compensator using the EIE-core variable inductor.

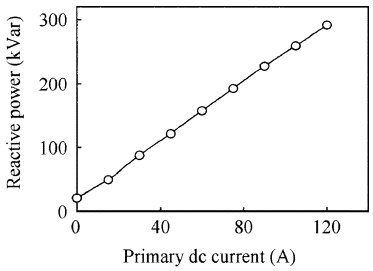

Fig. 9. Control characteristics of the reactive power.

III. Development of 300-kVA Reactive Power Compensator

Fig. 8 shows a general view of the trial three-phase 6.6-kV–300-kVA reactive power compensator using the EIE-core variable inductor. The oil-immersed and self-cooled system is adopted in the trial apparatus. The total weight of the apparatus, including control circuits, is 3.9 t.

Fig. 9 shows the control characteristics of the reactive power. It indicates that the trial apparatus has good controllability and a maximum capacity of 300 kVar.

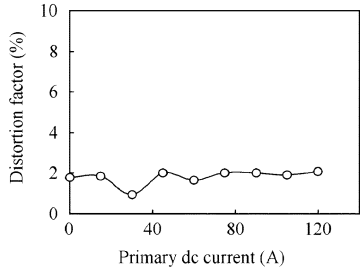

Fig. 10. Distortion factor of the secondary current.

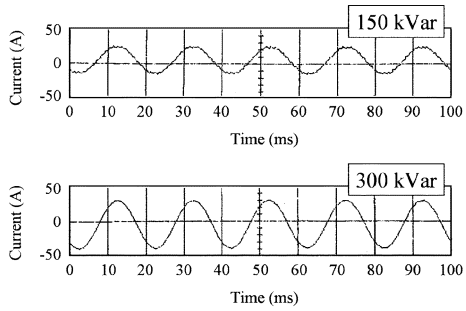

Fig. 11. Observed waveforms of the secondary current in half and full control conditions.

Fig. 10 demonstrates the distortion factor of the secondary current, and Fig. 11 shows the observed waveforms of the secondary current in half and full control conditions. The figures indicate that the trial apparatus has an almost sinusoidal output current in a wide control region.

IV. Conclusion

We presented an EIE-core suitable for a lager capacity variable inductor, and proposed a method for calculating the operating characteristics of the variable inductor including iron loss. It is understood that the characteristics of the variable inductor can be calculated accurately by using the RNA. It is particularly useful for optimum design of power apparatuses with very large capacity, since it is difficult to trial-manufacture such apparatuses.

We developed the trial 300-kVA reactive power compensator using the EIE-core. The trial apparatus has good controllability and an almost sinusoidal output current. We are now carrying out field tests of the trial reactive power compensator.

References

[1] L. Gyugyi, *IEEE Trans. Ind. Appl.*, vol. IA-15, no. 521, 1979.
[2] R. A. Best and H. Z. L. Parra, *IEEE Trans. Power Electron.*, vol. 11, no. 489, 1996.
[3] S. D. Wanlass, *IEEE Wescon Tech. Papers*, vol. 12, 1968.
[4] Z. H. Meiksin, *IEEE Trans. Ind. Appl.*, vol. 10, no. 417, 1974.
[5] K. Nakamura, O. Ichinokura, M. Maeda, S. Akatsuka, K. Takasugi, and H. Sato, *IEEE Trans. Magn.*, vol. 36, no. 3565, 2000.
[6] K. Tajima, A. Kaga, Y. Anazawa, and O. Ichinokura, *IEEE Trans. Magn.*, vol. 29, no. 3219, 1993.
[7] K. Tajima, Y. Anazawa, T. Komukai, and O. Ichinokura, *Eur. Power Electr. Conf.*, 1997, pp. 2.006–2.011.

Manuscript received February 7, 2005.